Advances in Nano Research, *Vol. 1, No. 4 (2013) 183-192*
DOI: http://dx.doi.org/10.12989/anr.2013.1.4.183

Fabrication of barium titanate-bismuth ferrite fibers using electrospinning

Avinash Baji*[1] and Mojtaba Abtahi[2a]

[1]*Engineering Product Development (EPD) Pillar, Singapore University of Technology and Design (SUTD), Singapore 138682, Singapore*
[2]*Centre for Advanced Materials Technology (CAMT), School of Aerospace, Mechanical and Mechatronic Engineering, University of Sydney, Sydney, NSW 2006, Australia*

(Received May 30, 2013, Revised October 17, 2013, Accepted October 20, 2013)

Abstract. One-dimensional multiferroic nanostructured composites have drawn increasing interest as they show tremendous potential for multifunctional devices and applications. Herein, we report the synthesis, structural and dielectric characterization of barium titanate ($BaTiO_3$)-bismuth ferrite ($BiFeO_3$) composite fibers that were obtained using a novel sol-gel based electrospinning technique. The microstructure of the fibers was investigated using scanning electron microscopy and transmission electron microscopy. The fibers had an average diameter of 120 nm and were composed of nanoparticles. X-ray diffraction (XRD) study of the composite fibers demonstrated that the fibers are composed of perovskite cubic $BaTiO_3$-$BiFeO_3$ crystallites. The magnetic hysteresis loops of the resultant fibers demonstrated that the fibers were ferromagnetic with magnetic coercivity of 1500 Oe and saturation magnetization of 1.55 emu/g at room temperature (300 K). Additionally, the dielectric response of the composite fibers was characterized as a function of frequency. Their dielectric permittivity was found to be 140 and their dielectric loss was low in the frequency range from 1000 Hz to 10^7 Hz.

Keywords: electrospinning; multiferroic; multifunctional; sol-gel; dielectric property; nano-fiber

1. Introduction

Materials that display multiple ferroic properties such as ferromagnetism and ferroelectricity have gained widespread interest due to their potential application in sensors, actuators, memory devices, microelectromechanical systems and spintronics (Bune *et al.*1998, Wang *et al.* 2003, Nan *et al.* 2008, Baji *et al.* 2011a, Baji *et al.* 2012, Baji *et al.* 2011b). Several materials such as oxide perovskites and sulfide spinels are reported to display ferromagnetism and ferroelectricity (Goto *et al.* 2005, Hemberger *et al.* 2005). Studies demonstrate that the oxide perovskites display a wide range of magnetic and electric properties including antiferromagnetic, antiferroelectric, and semiconductor behaviors and hence show tremendous potential for fabrication of multifunctional materials (Song *et al.* 2008, Xu *et al.* 2009).

Among all single phase perovskite structured materials bismuth ferrite ($BiFeO_3$) has attracted

*Corresponding author, Assistant Professor, E-mail: avinash_baji@sutd.edu.sg
[a]Ph.D., E-mail: mojtaba.abtahi@sydney.edu.au

Copyright © 2013 Techno-Press, Ltd.
http://www.techno-press.com/?journal=anr&subpage=7 ISSN: 2287-237X (Print), 2287-2388 (Online)

widespread attention as single crystals of $BiFeO_3$ are capable of demonstrating ferroelectric behavior below the Curie temperature (850℃) and ferromagnetic behavior below the Neel temperature (370℃) (Wang *et al.* 2003, Nan *et al.* 2008, Baji *et al.* 2011c). Further, $BiFeO_3$ in thin film form is found to display giant ferroelectric polarization value, which is reported to be ~150 $\mu C/cm^2$ at 90 K (Yun *et al.* 2006). However, the drawback of $BiFeO_3$ is its high level of electrical conductivity. The high level of electrical conductivity originates from the charged defects and oxygen vacancies, which makes it difficult to measure the dielectric and ferroelectric properties of $BiFeO_3$ at room temperature (Iakovlev *et al.* 2005). Further, the lower resistivity of $BiFeO_3$ leads to the display of magnetoelectric effect only at low temperatures.

Typical approach to suppress the leakage current and enhance its resistivity is to obtain a solid solution with other perovskite materials such as lead titanate ($PbTiO_3$) or barium titanate ($BaTiO_3$) (Kumar *et al.* 2000, Sakamoto *et al.* 2008). Previous studies (Kumar *et al.* 2000, Sakamoto *et al.* 2008) relied on chemical solution deposition to obtain composites such as $BiFeO_3$–$PbTiO_3$ and $BiFeO_3$-$BaTiO_3$ in thin film form. In this study, we use electrospinning to obtain $BiFeO_3$-$BaTiO_3$ in fiber form and demonstrate that electrospinning can be used successfully to obtain such nanostructured functional composites. BaTiO3 and PbTiO3 are commonly used as dopants and to suppress the leakage current of $BiFeO_3$ (Dutta *et al.* 1994, Buscaglia *et al.* 2006). Additionally, they have high dielectric constant and exhibit good ferroelectric behavior (Buscaglia *et al.* 2006, Baji *et al.* 2011a). Thus, combining $BaTiO_3$ and $BiFeO_3$ can yield composites that have low leakage current and that can exhibit ferromagnetism at ambient temperature. It is also known that the composites of $BiFeO_3$ and $BaTiO_3$ display well defined ferroelectric P-E hysteresis loops (Kumar *et al.* 2000, Sakamoto *et al.* 2008). Furthermore, the substitution of Fe sites with the Ti also leads to improve the magnetization of the composite. Such composites are highly useful as they not only display properties of the constituent materials but can also display magnetoelectric behavior arising from the interactions between the electric and magnetic orders (Nan *et al.* 2008). Wide range of techniques has been used to synthesize $BiFeO_3$-$BaTiO_3$ composites. Recent studies demonstrated that the reduced dimensionality afforded by the nanostructured composites can give rise to large magnetoelectric effect (Nan *et al.* 2005, Liu *et al.* 2006). This is attributed to the better coupling efficiency between the ferroelectric and ferromagnetic phases in nanostructured composites compared to their bulk counterparts. Thus, nanostructured composites open up the possibilities for discovering new class of multifunctional and multiferroic materials.

Electrospinning shows tremendous potential for fabrication of nanostructured fibers that are capable of displaying both ferroelectric and ferromagnetic behavior (Yuh *et al.* 2005, Zhu *et al.* 2006, Wu *et al.* 2007). Recently, we have successfully demonstrated that electrospinning combined with sol-gel technique can be used to fabricate nanostructured bismuth ferrite as well as barium titanate fibers (Baji *et al.* 2011a, c). Here, we go one step further and demonstrate that similar approach can be used to obtain barium titanate-bismuth ferrite composite fibers. These one-dimensional composite fibers show tremendous potential for their use as novel multiferroic materials in nanoscale devices and applications.

2. Experimental section

$BiFeO_3$-$BaTiO_3$ fibers were fabricated in this study using sol-gel enabled electrospinning technique. Precursor sol-gel solutions of $BiFeO_3$ and $BaTiO_3$ were prepared separately. Briefly, $BiFeO_3$ sol-gel named as Solution A was prepared by dissolving 3.03 g of $Fe(NO_3)_3 \cdot 9H_2O$ and 4 g

of of $Bi(NO_3)_3 \cdot 5H_2O$ in 10 ml of 2-methoxyethanol and 5 ml of glacial acetic acid solution mixture. In the next step, $BaTiO_3$ precursor solution named as Solution B was prepared by dissolving 2.55 g of barium acetate in 6 ml of acetic acid and 2.95 ml of titanium isopropoxide solution mixture. The detailed descriptions for the preparation of $BiFeO_3$ sol-gel and $BaTiO_3$ sol-gel are given in our previous studies (Baji *et al.* 2011a,c).

2.1 Electrospinning

To prepare the electrospinning solution, the prepared Solution A was added to the 15 ml of ethanol solution under constant stirring condition. Following this, Solution B of known quantity was added to the above solution such that the molar ratio between $BiFeO_3$ and $BaTiO_3$ was 6:4. Once homogenous solution was obtained, 2 g of polyvinyl pyrrolidone (PVP) with molecular weight 360,000 was added to the solution and stirred until PVP was completely dissolved. Electrospinning was then conducted at 21 kV and the flow rate of the solution was 0.07 mm/min. 15 cm spacing was used between the tip of the needle and the collector surface.

Neat $BiFeO_3$ fibers and neat $BaTiO_3$ fibers were also fabricated for comparison purposes. Identical quantity of Solution A and Solution B as used for composite fiber preparation was added separately to the 15 ml of ethanol solution. 2 g of PVP with molecular weight 360,000 was added to the solutions and stirred. Following this, electrospinning was conducted at 21 kV and flow rate was set at 0.07 mm/min to obtain neat $BiFeO_3$ fibers and neat $BaTiO_3$ fibers.The collected fibers were dried in an oven at 100 ℃ for 24 h duration. The dried fibers were then transferred into a furnace for thermal annealing. The fibers were heated from ambient temperature to 750℃. The heating rate was 5℃/min and the dwelling time at 750℃ was 1 h.

2.2 Microstructure characterization

The morphology of the fibers was analysed using a field emission scanning electron microscope (FESEM, Zeiss ULTRA *plus*). The obtained fibers before and after the thermal annealing procedure were coated with a thin layer of gold and were then examined using a SEM at an accelerating voltage of 5 kV. Transmission electron microscopy (TEM, Philips CM120 Biofilter) was used to examine the fibers.

2.3 X-ray diffraction (XRD)

The crystal structures of the fibers were determined from the XRD patterns. XRD patterns of pure $BiFeO_3$ and pure $BaTiO_3$ fibers were used for comparison purpose. XRD was conducted in reflection mode at ~ 25℃ using a X-ray diffractometer (XRD Shimadzu S6000) with CuKα radiation (λ=1.54 Å). The 2θ scan was varied between 15° and 70° and the scan speed was set at 1 °/min with 0.02° step size.

2.4 Ferromagnetic behavior

The ferromagnetic hysteresis loops of the fibers were measured at room temperature using a commercial Quantum Design magnetic property measurement system (MPMS) and physical property measurement system (PPMS). A vibrating sample method was used to obtain the

magnetic hysteresis curves. The magnetic field was ramped at ambient temperature (300 K) from 10,000 Gauss to −20,000 Gauss and back to 20,000 Gauss.

2.5 Dielectric behavior

For electrical property characterization, the $BiFeO_3$-$BaTiO_3$ fibers were ground and broken into shorter fragments. The fragments were then pressed together to obtain disk shaped specimen. Following this, the disk shaped specimen was sintered at 950℃ for 1 h. Silver paint was coated on both the sides of the specimen, which served as electrodes. The dielectric permittivity and loss tangent (Tan δ) were measured as a function of frequency using a HP4294A impedance analyzer, which is controlled by a computer.

3. Results and discussion

Electrospinning the precursor sol-gel solution of barium titanate-bismuth ferrite along with PVP solution lead to the formation of the precursor fibers. Fig. 1 shows the morphology of the barium titanate-bismuth ferrite precursor fibers. It is evident from Fig. 1 that the precursor fibers have smooth morphology and uniform diameter.

The average diameter of these fibers is determined to be ~350 ± 120 nm. The fibers are then thermally annealed in a furnace at 750℃. Thermal annealing led to the removal of the organic PVP phase and also promoted the crystallization of the inorganic phases within the fiber geometry. The resultant fibers are $BaTiO_3$-$BiFeO_3$ fibers. Fig. 2 shows representative SEM micrograph of $BaTiO_3$-$BiFeO_3$ fibers obtained after the thermal treatment. As evident from Fig. 2, the obtained fibers are composed of compact and uniform microstructures. The fibers have a wide distribution of size, ranging from 32 nm to 200 nm diameter. The average diameter of the fibers is determined to be 100 nm ± 50 nm. It is clear from the SEM images that the fibers are composed of nanostructured grains.

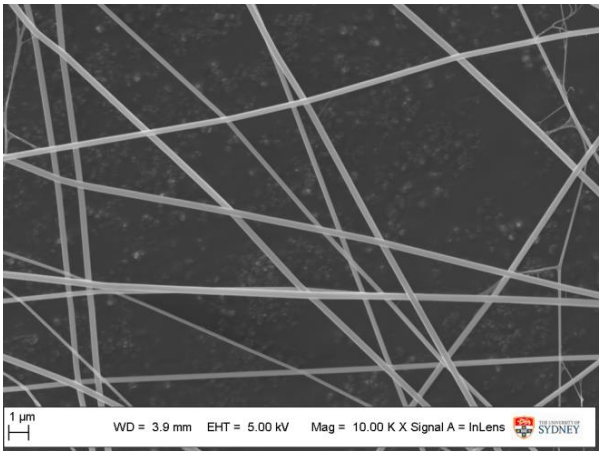

Fig. 1 SEM photomicrograph of precursor fibers obtained by electrospinning precursor sol-gel solution mixed with PVP solution

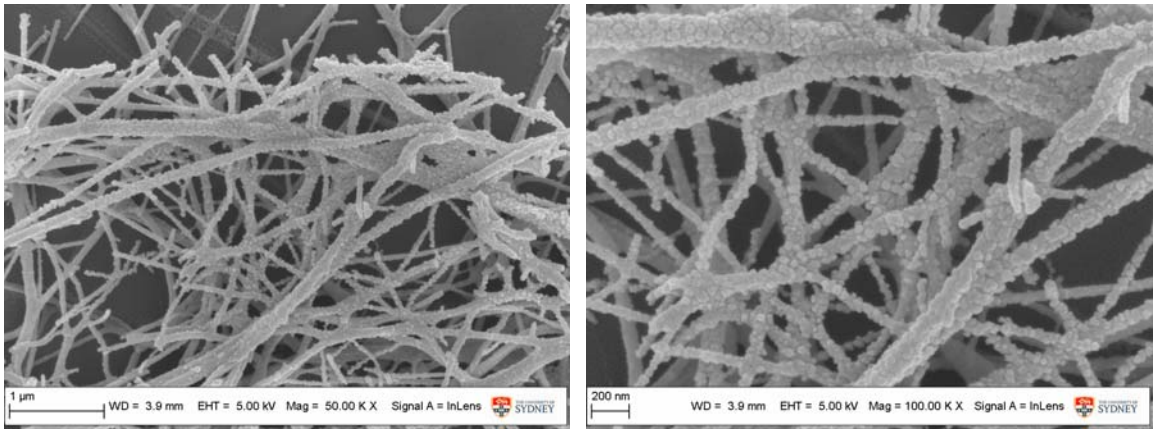

(a) Low magnification image

(b) High magnification image demonstrating the self-organization and arrangement of the particles within the fibrous geometry

Fig. 2 SEM images of barium titanate-bismuth fibers. These fibers are obtained after thermally treating the precursor fibers

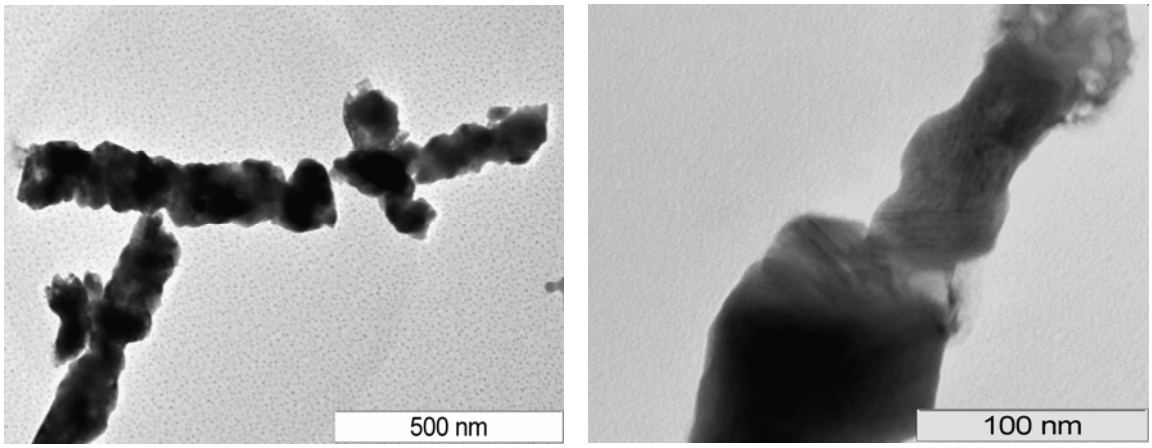

(a) Low magnification image

(b) High magnification image

Fig. 3 TEM image of the barium titanate-bismuth ferrite fibers

The fiber morphology consists of nanoparticles that are self-assembled and connected together to yield fibrous geometry. The sizes of the particles are characterized based on the SEM images and their average diameter is determined to be 40 nm ± 11 nm. These nanostructured particles are well-interlinked, self-assembled and randomly oriented within the fibrous geometry. The reduction in the size of the fibers after thermal treatment is due to the removal of the polymer phase from the fibers.

Fig. 3 shows the TEM images of the thermally annealed fibers. The fibers after the thermal treatment are dispersed in an ethanol solution followed by sonication. This process breaks the

fibers into shorter fragments. Once the fibers are homogeneously dispersed in the ethanol solution, a pipette is used to place a drop of ethanol solution on TEM grids. Thus, individual fibers and shorter fragments of fibers can be imaged using TEM. The TEM images are used to analyse the shape, size and arrangement of the particles. The TEM images shown in Fig. 3 demonstrate that the inorganic particles within the fibrous geometry are self-assembled and self-organized. An image-analysing software ImageJ is used to study the size distribution and average size of the particles. Consistent with the SEM results, the sizes of the particles are found to be ~42 nm in diameter.

Following this, the thermal evolution and crystalline formation of the $BaTiO_3$-$BiFeO_3$ phases are monitored using XRD. XRD peaks of the fibers thermally annealed at 750℃ are presented in Fig. 4. XRD peaks of neat $BiFeO_3$ and neat $BaTiO_3$ are also shown in Fig. 4 for comparison purpose. Neat $BaTiO_3$ fibers as well as neat $BiFeO_3$ fibers show clear distinct peaks, which indicate the polycrystalline nature of both the fibers. The XRD peaks of the neat bismuth ferrite fibers match the XRD peaks of the rhombohedral distorted perovskite structure reported in literature for pure bismuth ferrite. The peaks of bismuth ferrite fibers closely match with the pure bismuth ferrite (JCPDS 86-1518) (Sahu 2007). Similarly, the XRD profile of pure barium titanate fibers is characterized by clear and intense peaks. The XRD profile of these fibers matches closely with the cubic and tetragonal phases (JCPDS 31-0174 and JCPDS 05-0626 respectively) of pure barium titanate phase (Lee *et al.* 2012). Barium titanate is identified to exist in the tetragonal structure if its peaks at 56.3 and 66.1° demonstrate splitting. Although not clearly visible in Fig. 4, the XRD peaks of neat barium titanate fibers splits at 56.3 and 66.1°, indicating the tetragonal structure of the fabricated fibers.

It is clear from Fig. 4 that the characteristic peaks attributed to the crystalline bismuth ferrite and barium titanate fibers are also evident in the XRD profile of barium titanate-bismuth ferrite

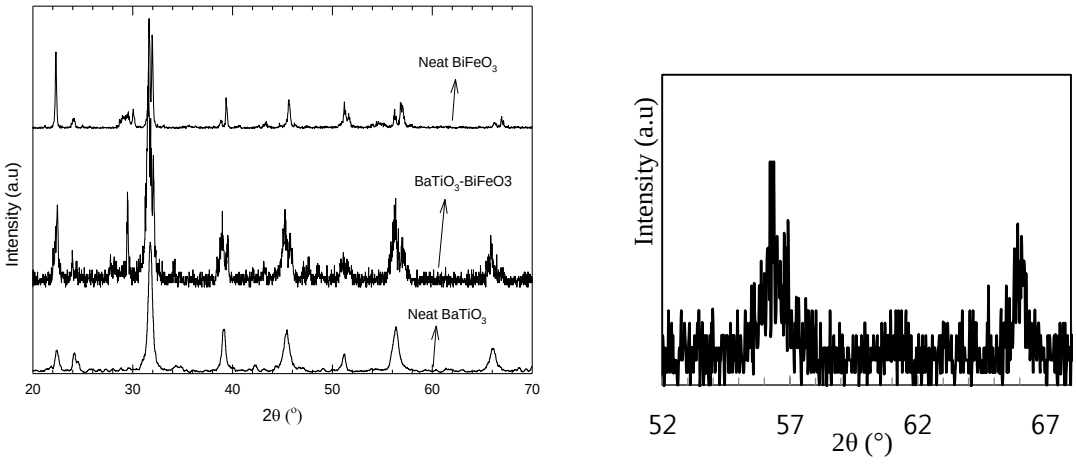

(a) XRD peaks of neat $BiFeO_3$, neat $BaTiO_3$ and $BiFeO_3$-$BaTiO_3$ fibers

(b) Expanded view of $BaTiO_3$ XRD curve demonstrating the splitting of peaks

Fig. 4 XRD peaks of the barium titanate-bismuth ferrite fibers. XRD peaks of neat barium titanate and neat bismuth ferrite fibers are also shown for comparison purposes

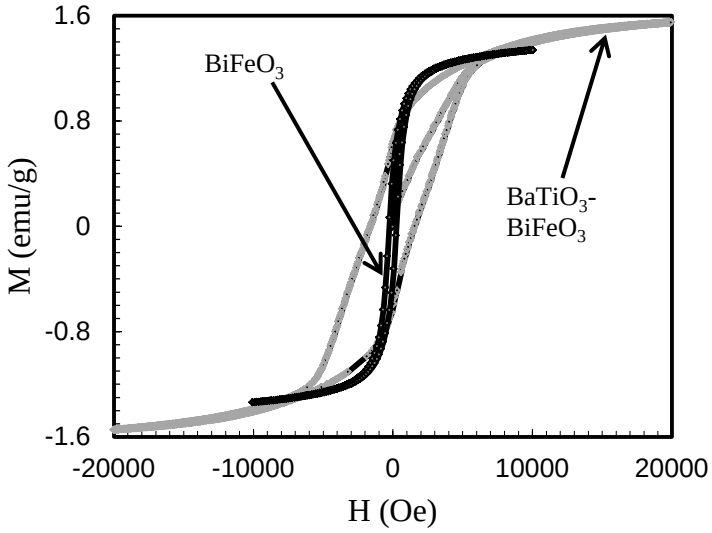

Fig. 5 Magnetization versus applied magnetic field (*M-H*) hysteresis loops of barium titanate-bismuth ferrite fibers. The *M-H* hysteresis loops of neat bismuth ferrite fibers are also shown for comparison. The measurements are made at ambient temperature (~300K)

composite fibers. It is clear that the peaks for the composite fibers shows splitting, which indicates that the composite fibers is characterized by both rhombohedral and cubic structure. The XRD peaks of the composite fibers indicate that the bismuth ferrite retains its rhombohedral pervoskite structure and barium titanate retains its cubic tetragonal structure in the composite. Thus, the XRD peaks demonstrate that both barium titanate and bismuth ferrite phases co-exist after the thermal annealing process in the composite fibers. All the peaks are identified for the composite fibers with no interfacial phases. This indicates that thermal treatment of the precursor fibers yields barium titanate and bismuth ferrite fibers and no chemical interaction has occurred between the two phases during the thermal annealing process.

The magnetic hysteresis loops of the composite fibers recorded at ambient temperature is shown in Fig. 5. For comparison, the magnetic hysteresis loops of neat bismuth ferrite fibers are also shown. Interestingly, magnetization of both samples shows hysteretic dependence on the external magnetic field. This hysteresis behavior of both samples is completely different compared to the bulk polycrystalline bismuth ferrite (Iakovlev *et al.* 2005). Bulk polycrystalline bismuth ferrite samples do not demonstrate any hysteresis loops as they are associated with a disproportionate spiral spin structure (Wang *et al.* 2003, Baji *et al.* 2011c). This disproportionate spiral spin structure is responsible for cancelling its macroscopic magnetization.

However, both fiber systems obtained in this study display hysteresis behavior and ferromagnetism which can be attributed to the nanometer length scale of the fibers (Nan *et al.* 2005, Baji *et al.* 2011c). In both systems, the fibers are made of nano sized particles that are arranged to yield fibrous geometry. It is known that when the size of the particles is lower than the size of spiral ordering, the sample can display clear hysteresis loops and ferromagnetism (Mazumder *et al.* 2007). The particles in both systems are smaller than the size of the spiral ordering. This suggests that large fraction of the atoms within the particles are located at the

surface of the particles and grain boundaries. The magnetization of the fibers is influenced by the interface spins in the grains and gives rise to canted spin structures. Thus, the samples demonstrate hysteretic behavior.

It is interesting to note that the magnetic behavior of the composite fibers is different compared to the magnetic behavior displayed by neat bismuth ferrite fibers. As evident, the hysteresis loops of the composite fibers fully saturate at a high magnetic field of 20 kOe. On the contrary, the hysteresis loops of neat bismuth ferrite fibers saturate at much lower magnetic field of 10 kOe. Spontaneous magnetization (M_s) and coercivity (H_c) of the composite fibers and neat bismuth ferrite fibers is determined from the hysteresis loops. M_s and H_c values of neat bismuth ferrite fibers are found to be 1.32 emu/g and 250 Oe respectively. These values are lower than the M_s and H_c values of composite fibers which are found to be 1.53 emu/g and 1500 Oe respectively. The improvement of saturation magnetization in these composites can be attributed to the presence of barium titanate phase which promotes ferromagnetism in the bismuth ferrite phase (Kumar *et al.* 2000, Liu *et al.* 2006). The lattice constraints and interface diffusion of the barium titanate leads to continuing collapse of the spin structures. Thus, there is improved canting effect in the composite fibers due to structural distortions (Quan *et al.* 2008). This explains the improvement of the magnetization seen in composite fibers compared to neat bismuth ferrite fibers. The improvement of magnetization due to inclusion of ferroelectric barium titanate phase shows great potential of these composites for magneto-electric applications.

In the next step, we investigate the frequency dependence of dielectric permittivity and dielectric loss of the barium titanate-bismuth ferrite composite fibers. Fig. 6 shows the permittivity and dielectric loss as a function of frequency for the composite fibers. It is evident from Fig. 6 that the dielectric permittivity and dielectric loss for the sample is dependent on the frequency. The dielectric permittivity of the sample decreases as the frequency is increased. This trend of decreasing permittivity with frequency can be explained using the dipole relaxation phenomenon (Singh *et al.* 2011). The inability of the electric dipoles to switch with the frequency of applied electric field explains the reason for lower permittivity values at higher frequencies. Further, it is

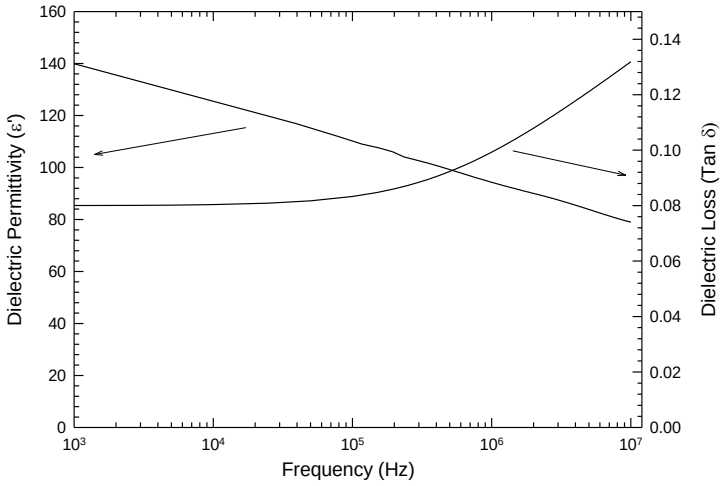

Fig. 6 Frequency dependence of dielectric permittivity and dielectric loss for composite fibers

known that at low frequencies, the dielectric permittivity is influenced by varies types of polarizations such as ionic, electronic, interfacial and atomic. However, at high frequencies, the dielectric permittivity is only influenced by the electronic polarizations. This explains the lower dielectric permittivity values of the sample at higher frequencies.

It is well known that the dielectric constant of barium titanate is higher than that of bismuth ferrite. This suggests that dielectric constant of composite composed of barium titanate and bismuth ferrite will be higher than that of neat bismuth ferrite. Thus, this system shows tremendous potential for use in dielectric applications. It is evident from Fig. 6 that the dielectric loss measured for the sample is more or less constant at lower frequencies and tend to increase as the frequency is increased above 10^5 Hz. This indicates that the spectrum shows relaxation at 10^5 Hz frequency.

5. Conclusions

We have used electrospinning combined with sol-gel technique to successfully fabricate barium titanate-bismuth ferrite fibers. We demonstrate that the obtained composite fibers consist of fine particles that self-assemble to yield a fibrous geometry. X-ray diffraction profile of the sample demonstrated the presence of polycrystalline structure with characteristic peaks of both bismuth ferrite and barium titanate phase. This demonstrates that the obtained fibers were composed of both the phases. The magnetization of the composite fiber is found to be higher than that of neat bismuth ferrite fibers. This is attributed to the presence of barium titanate phase which improves the magnetization of the fibers. The improvement in the magnetization of the sample with the addition of ferroelectric barium titanate shows tremendous potential of using this technique for fabricating magnetoelectric composites. Experiments are in progress to determine the magnetoelectric properties of such composites.

References

Baji, A., Mai, Y.W., Du, X.S. and Wong, S.C. (2012), "Improved tensile strength and ferroelectric phase content of self-assembled polyvinylidene fluoride fiber yarns", *Macromol. Mater. Eng.*, **297**(3), 209-213.

Baji, A., Mai, Y.W., Li, Q. and Liu, Y. (2011a), "Nanoscale investigation of ferroelectric properties in electrospun barium titanate/polyvinylidene fluoride composite fibers using piezoresponse force microscopy", *Compos. Sci. Technol.*, **71**(11), 1435-1440.

Baji, A., Mai, Y.W, Li, Q. and Liu, Y. (2011b), "Electrospinning induced ferroelectricity in poly (vinylidene fluoride) fibers", *Nanoscale*., **3**(8), 3068-3071.

Baji, A., Mai, Y.W., Li, Q.A., Wong, S.C., Liu, Y. and Yao, Q.W. (2011c), "One-dimensional multiferroic bismuth ferrite fibers obtained by electrospinning techniques", *Nanotechnology*, **22**(23), 235702.

Bune, A.V., Fridkin, V.M., Ducharme, S., Blinov, L.M., Palto, S.P., Sorokin, A.V., Yudin, S.G. and Zlatkin, A. (1998), "Two-dimensional ferroelectric films", *Nature*, **391**(6670), 874-877.

Buscaglia, M.T., Viviani, M., Buscaglia, V., Mitoseriu, L., Testino, A., Nanni, P., Zhao, Z., Nygren, M., Harnagea, C., Piazza, D. and Galassi, C. (2006), "High dielectric constant and frozen macroscopic polarization in dense nanocrystalline BaTiO3 ceramics", *Phys. Rev. B*, **73**(6), 064114.

Dutta, P.K., Asiaie, R., Akbar, S.A. and Zhu, W.D. (1994), "Hydrothermal synthesis and dielectric-properties of tetragonal $BaTiO_3$", *Chem. Mater.*, **6**(9), 1542-1548.

Goto, T., Yamasaki, Y., Watanabe, H., Kimura, T. and Tokura, Y. (2005), "Anticorrelation between

ferromagnetism and ferroelectricity in perovskite manganites", *Phys. Rev. B*, **72**(22), 220403.
Hemberger, J., Lunkenheimer, P., Fichtl, R., von Nidda, H.A.K., Tsurkan, V. and Loidl, A. (2005), "Relaxor ferroelectricity and colossal magnetocapacitive coupling in ferromagnetic CdCr2S4", *Nature*, **434**(7031), 364-367.
Iakovlev, S., Solterbeck, C.H., Kuhnke, M. and Es-Souni, M. (2005), "Multiferroic BiFeO3 thin films processed via chemical solution deposition: Structural and electrical characterization", *J. App. Phys.*, **97**(9), 094901.
Kumar, M.M., Srinivas, A. and Suryanarayana, S.V. (2000), "Structure property relations in BiFeO3/BaTiO3 solid solutions", *J. App. Phys.*, **87**(2), 855-862.
Lee, H.W., Moon, S., Choi, C.H. and Kim, D.K. (2012), "Synthesis and size control of tetragonal barium titanate nanopowders by facile solvothermal method", *J. Am. Ceram. Soc.*, **95**(8), 2429-2434.
Liu, G., Nan, C.W. and Sun, J. (2006), "Coupling interaction in nanostructured piezoelectric/magnetostrictive multiferroic complex films", *Acta Mater.*, **54**(4), 917-925.
Mazumder, R., Devi, P.S., Bhattacharya, D., Choudhury, P., Sen, A. and Raja, M. (2007), "Ferromagnetism in nanoscale BiFeO3", *Appl. Phys. Lett.*, **91**(6), 062510.
Nan, C.W., Bichurin, M.I., Dong, S.X., Viehland, D. and Srinivasan, G. (2008), "Multiferroic magnetoelectric composites: Historical perspective, status, and future directions", *J. Appl. Phys.*, **103**(3), 031101.
Nan, C.W., Liu, G., Lin, Y.H. and Chen, H.D. (2005), "Magnetic-field-induced electric polarization in multiferroic nanostructures", *Phys. Rev. Lett.*, **94**(19), 197203.
Quan, Z.C., Liu, W., Hu, H., Xu, S., Sebo, B., Fang, G.J., Li, M.Y. and Zhao, X.Z. (2008), "Microstructure, electrical and magnetic properties of Ce-doped BiFeO(3) thin films", *J. Appl. Phys.*, **104**(8), 084106.
Sahu, J.R. (2007), "Beneficial modification of the properties of multiferroic BiFeO3 by cation substitution", *Solid State Sci.*, **9**(10), 950-954.
Sakamoto, W., Iwata, A. and Yogo, T. (2008), "Ferroelectric properties of chemically synthesized perovskite BiFeO3-PbTiO3 thin films", *J. Appl. Phys.*, **104**(10), 104106.
Singh, H., Kumar, A. and Yadav, K.L. (2011), "Structural, dielectric, magnetic, magnetodielectric and impedance spectroscopic studies of multiferroic BiFeO3-BaTiO3 ceramics", *Mater. Sci. Eng. B-Adv. Funct. Solid-State Mater.*, **176**(7), 540-547.
Song, C., Wang, C.Z., Yang, Y.C., Liu, X.J., Zeng, F. and Pan, F. (2008), "Room temperature ferromagnetism and ferroelectricity in cobalt-doped LiNbO(3) film", *Appl. Phys. Lett.*, **92**(26), 262901.
Wang, J., Neaton, J.B., Zheng, H., Nagarajan, V., Ogale, S.B., Liu, B., Viehland, D., Vaithyanathan, V., Schlom, D.G., Waghmare, U.V., Spaldin, N.A., Rabe, K.M., Wuttig and M., Ramesh, R. (2003), "Epitaxial BiFeO3 multiferroic thin film heterostructures", *Science*, **299**(5613), 1719-1722.
Wu, H., Zhang, R., Liu, X.X., Lin, D.D. and Pan, W. (2007), "Electrospinning of Fe, Co, and Ni nanofibers: Synthesis, assembly, and magnetic properties", *Chem. Mater.*, **19**(14), 3506-3511.
Xu, B., Yin, K.B., Lin, J., Xia, Y.D., Wan, X.G., Yin, J., Bai, X.J., Du, J. and Liu, Z.G. (2009), "Room-temperature ferromagnetism and ferroelectricity in Fe-doped BaTiO3", *Phys. Rev. B*, **79**(13), 134109.
Yuh, J., Nino, J.C. and Sigmund, W.A. (2005), "Synthesis of barium titanate (BaTiO3) nanofibers via electrospinning", *Mater. Lett.*, **59**(28), 3645-3647.
Yun, K.Y., Ricinschi, D., Kanashima, T. and Okuyama, M. (2006), "Enhancement of electrical properties in polycrystalline BiFeO3 thin films", *Appl. Phys. Lett.*, **89**(19), 192902.
Zhu, Y., Zhang, J.C., Zhai, J. and Jiang, L. (2006), "Preparation of superhydrophilic alpha-Fe2O3 nanofibers with tunable magnetic properties", *Thin Solid Films*, **510**(1-2), 271-274.

CC